JOURNAL OF Materials CHEMISTRY

Cobalt–zinc oxide absorbents for low temperature gas desulfurisation

Thomas Baird,[a] Kenneth C. Campbell,[a] Peter J. Holliman,[a] Robert W. Hoyle,[a] Max Huxam,[a] Diane Stirling,*[a] B. Peter Williams[b] and Michael Morris[c]

[a] *Chemistry Department, University of Glasgow, Glasgow, UK G12 8QQ*
[b] *ICI Katalco, Billingham, UK Cleveland*
[c] *University College Cork, Ireland*

Received 4th September 1998, Accepted 7th October 1998

The hydrogen sulfide absorption capacity of a series of cobalt–zinc oxides with nominal Co/Zn atomic ratios of 0/100, 10/90, 20/80, 30/70, 40/60, 50/50, 70/30, 90/10 and 100/0 was determined using a continuous flow absorption apparatus. The reaction of the mixed oxides with H_2S amounted to *ca.* 3 monolayers, and is therefore largely confined to the surface of the oxides. The sulfur uptake was found to be proportional to the surface area of the oxides with a Co/Zn ratio $\leqslant$40/60, indicating that lattice diffusion played a major role in the rate determining step, and that the main function of the cobalt was to increase the surface area. At high cobalt concentrations, the sulfur uptake increased more than proportionately with surface area and the reaction was virtually stoichiometric for the oxide with a Co/Zn ratio of 100/0. This was associated with a change in the oxide structure from a bulk biphasic ZnO and Co_3O_4 absorbent with a $ZnCo_2O_4$ surface spinel at Co/Zn ratios $\leqslant$70/30 to a monophasic zincian or pure Co_3O_4 structure at higher cobalt loadings. Analysis of the sulfided mixed oxides showed that microcrystalline membraneous sheets containing cobalt, zinc and sulfur developed on sulfiding. XPS studies of the sulfided oxides indicated that H_2S reduced the surface spinel found at Co/Zn ratios $\leqslant$30/70 and the zincian/pure Co_3O_4 found at higher cobalt concentrations to CoO and ZnO prior to the formation of their sulfides. The results are interpreted in terms of a surface reconstruction occurring during sulfiding.

Introduction

H_2S, COS, mercaptans and other sulfur-containing organic compounds are found as natural contaminants in many industrially important hydrocarbon feedstocks. There are clear economic and environmental benefits to be gained by reducing the sulfur content of feedstocks to less than ppm levels. Thus, for example, hydrocarbon feedstocks are used in the manufacture of both high tonnage and high value chemicals. Many of these employ supported metal catalysts that are easily poisoned by sulfur compounds,[1] and sulfur levels in excess of 3 ppm in feedstocks can also limit plant lifetime by causing pipeline corrosion. Sulfur in the feedstock therefore makes frequent catalyst and pipeline replacement necessary, and this adds considerably to the cost of chemical manufacture. Furthermore, sulfur compounds retained in feedstocks during processing can also contribute to acid rain when emitted into the atmosphere[2] so there are clear environmental advantages in efficient desulfurisation of feedstocks and clean-up of refinery effluent.

Sulfur removal from feedstocks generally involves the initial conversion of sulfur-containing organics to H_2S using a $CoO/MoO_3/Al_2O_3$ catalyst at 643 K, 40 bar, followed by removal of the H_2S in a bed of highly porous zinc oxide at 350–450 °C.[3] Although the use of metal oxides for high temperature (>300 °C) sulfur removal has been widely studied,[4–6] low temperature sulfur removal has received little attention. The first H_2S absorbents used at ambient temperature were hydrated iron oxides which were used for the absorption of H_2S produced from coal gas.[7,8] However, iron sulfide is pyrophoric and iron oxide has therefore been largely replaced in Europe by zinc oxide as an absorbent.[9,10] Although the absorption of H_2S by ZnO is stoichiometric at 350 °C, it falls off rapidly at lower temperatures. A number of absorbents have now been developed with improved absorption capacity including a high surface area zinc oxide,[3] iron, copper and cobalt doped zinc oxide,[11] and feroxyhyte (FeOOH),[12] cobalt–zinc and cobalt–zinc–aluminium mixed oxides.[13,14] In our studies, the Co/Zn mixed oxides were the best absorbents for sulfur removal. In a previous paper we reported the characterisation of a series of Co–Zn hydroxycarbonates and their decomposition products,[15] and their use as absorbents for low temperature gas desulfurisation is described in this paper.

Experimental

Absorbent preparation

Precursors with nominal atomic ratios of Co/Zn 0/100, 10/90, 20/80, 30/70, 40/60, 50/50, 70/30, 90/10 and 100/0 were prepared by coprecipitation at low supersaturation and a constant pH of 7 as previously described.[15] The precursors were dried in an oven at 110 °C for 16 h and calcined, as a finely ground powder, in a muffle oven at 350 °C for 16 h.[15] The finely powdered oxides were pressed into discs, crushed and sieved to particle sizes of 500–1000 μm prior to use as absorbents.

Characterisation of sulfided absorbents

Transmission electron microscopy (TEM). The samples were examined on either a JEOL 1200X or a JEOL-100C transmission electron microscope. Selected samples were also examined using an ABT-EM002B microscope in which an energy dispersive X-ray spectroscopy (EDX) system was installed. Specimens were prepared by grinding them to a fine powder, suspending them in water and then mounting them on carbon-filmed copper grids.

IR spectroscopy (FTIR). The spectra of the powdered samples were obtained as KBr discs using a Philips PU980 FTIR spectrometer in transmission mode, between 4000 and 400 cm^{-1}.

Electron energy loss spectroscopy (EELS). EELS studies were carried out on selected samples using a Zeiss 902 microscope fitted with electron spectroscopic imaging equipment.

X-Ray photoelectron spectroscopy (XPS). *Qualitative analysis.* X-Ray photoelectron spectra were obtained using Al-Kα ($h\nu = 1486.6$ eV; 1 eV $= 1.602 \times 10^{-19}$ J) monochromatized radiation with a Surface Science Instruments M-Probe spectrometer connected to a Hewlett Packard Vectra RS/20C computer for data acquisition and analysis. The analysis chamber was evacuated to better than 1×10^{-8} Torr before running the spectra. The spectra were recorded at room temperature and at low X-ray fluxes (anode operating at 10 kV and 22 mA). The data analysis procedure generally involved background subtraction by a Shirley-type integral profile and a curve fitting procedure by a least-squares method.

The spectra were analyzed in terms of the relative peak area intensities, the full-width at half-maximum height (FWHM) of the peaks, the chemical shifts of the $2p_{3/2}$ transitions of zinc and cobalt, and the oxygen 1s transition. Spectra were collected with a pass energy of 50 eV. The experimental errors were estimated to be ± 0.2 eV for the photoelectron peak binding energy positions.

The samples were loaded using double-sided Scotch tape. A low energy electron-flood gun was used and residual charging effects were corrected for all the samples. The sulfided oxides were charge referenced to the O 1s peak at $E_B = 530.0$ eV. It is appreciated by the authors that the chemical environment within the series of sulfided oxides will vary and hence affect the true position of the O 1s peak. The O 1s peak was chosen for the sulfides so that the oxide binding energies of the sulfided samples could be compared with those obtained for the unsulfided samples reported previously.[15]

Quantitative analysis. The surface Co/S and Zn/S ratios were calculated using eqn. (1).

$$\frac{n_S}{n_M} = \frac{I_S}{I_M} \times \frac{\alpha_M}{\alpha_S}\left(\frac{E_M}{E_S}\right)^{0.75} \quad (1)$$

In eqn. (1), n_M are the number of metal atoms at the surface, where M = Zn or Co, I_M and I_S are the intensities of zinc/cobalt and sulfur, respectively, α_M and α_S are the photoionisation cross-sections of the respective elements and E_M and E_S are the kinetic energies of the respective elements. The justification for using eqn. (1) to calculate the surface Co/S and Zn/S ratios has been presented by us previously in a paper describing the characterisation of the oxides by XPS.[15] The ratios of the photoionisation cross-sections, α_{Zn}/α_S and α_{Co}/α_S were taken from Schofield[16] and were found to be 11.28 and 7.53 respectively. The kinetic energy values for each element were calculated from the binding energy values of the atom obtained from Briggs and Seah.[17] The ratios were found to be 0.351 for Zn/S and 0.534 for Co/S. As stated in our previous paper,[15] we appreciate that absolute binding energies are difficult to determine because of the problems of charge referencing, and quantitative surface analysis is difficult due to the presence of an Auger transition in the Co $2p_{3/2}$ spectral region which causes the absolute Co $2p_{3/2}$ integrated intensity to be overestimated by 15%.[18] Therefore, the aim of this work was not to obtain absolute values but rather identify any trends that were present.

Absorbent testing

The H_2S absorption capacities of the sieved Co/Zn oxide absorbents were tested using the continuous flow microreactor described previously.[14] In a typical experiment a stream of 2% H_2S–N_2 was passed through a 5 cm^3 bed of absorbent particles, and the time required for breakthrough of H_2S from the bed was determined by the detection of 2–3 ppm H_2S in the exit stream measured by the precipitation of lead sulfide from an alkaline lead acetate solution. The concentration of H_2S in the feed stream was determined by GC analysis.

Table 1 H_2S absorption 'breakthrough' test data

Co/Zn			H_2S		
Nominal	Actual	S/ m^2 g^{-1}	adsorbed/ 10^{-5} mol m^{-2}	% Reaction	Reaction depth/ monolayers
0/100	0/100	38.8	4.353	13.73	2.6
10/90	11/89	45.1	4.943	20.46	2.8
20/80	26/74	64.9	4.514	23.86	2.4
30/70	31/69	68.2	4.983	28.58	2.5
40/60	44/56	66.4	5.570	33.18	2.6
50/50	46/54	59.7	3.907	20.07	1.8
70/30	75/25	56.5	8.138	46.22	3.1
90/10	91/9	82.9	9.193	63.11	3.0
100/0	100/0	87.1	12.412	91.82	3.7

Results

Bulk analysis

The total uptake of H_2S at breakthrough for 5 cm^3 of each absorbent was determined from the measured flow rate of H_2S–N_2 and the time required for breakthrough. The extent of reaction was then determined from the ratio of the number of moles of H_2S absorbed to the total number of moles of metal in the absorbent. The results obtained for each absorbent are listed in Table 1. The composition of each of the oxides was determined by atomic absorption as stated previously.[15] In general, there was good agreement between the nominal and expected Co/Zn ratios, so the nominal loadings will be quoted in the text. The actual metal loadings are included in Table 1 for comparison.

The % reaction has been plotted against the surface areas of the oxides in Fig. 1. For oxides with Co/Zn compositions ranging from 0/100 up to 40/60, only a slight dependence of the % reaction against surface area was observed, the % reaction being approximately proportional to the surface area. This trend was more clearly defined in a plot of % reaction against % cobalt concentration (Fig. 2). The % reaction and surface area were both lower than expected in the case of the Co/Zn 50/50 absorbent. For Co/Zn compositions 70/30, 90/10 and 100/0, the % reaction increased markedly with increase in surface area and % cobalt concentration. This indicated that the mechanism of sulfiding the oxides with a low Co/Zn ratio, which adopted a hexagonal zinc oxide based structure, was different from that found at high Co/Zn ratios where the oxides adopted the Co_3O_4 spinel structure.[15]

Transmission electron micrographs of selected sulfided oxides are shown in Fig. 3. A comparison with the micrographs of the oxides reported previously[15] showed that all the samples, with the exception of the Co/Zn 0/100 oxide, were comprised of particles that had increased in size and become semi-fused. Before sulfiding, the particles ranged from *ca.* 20–50 nm in size,[15] but it was not possible to determine accurately their

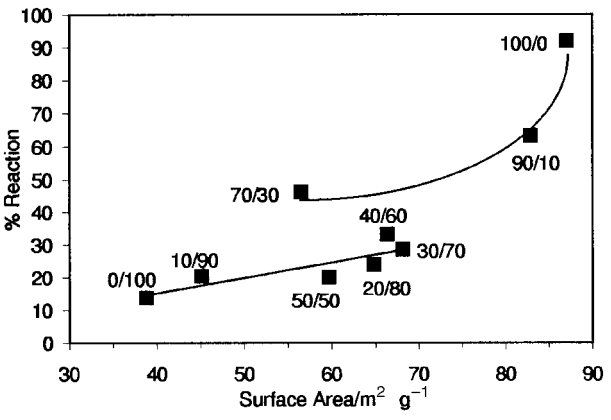

Fig. 1 Plot of % reaction against surface area for the sulfided oxides.

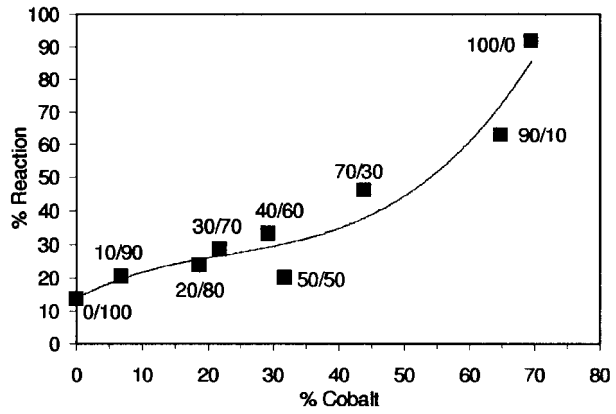

Fig. 2 Plot of % reaction against % cobalt for the sulfided oxides.

size after sulfiding due to their fused appearance. It should also be noted that all the samples containing both cobalt and zinc had very thin sheets of material around the sides of the semi-fused particles. No sheet-like material was observed in any of the oxides before sulfiding, or in the sulfided Co/Zn 0/100 or 100/0 samples. Energy dispersive X-ray spectroscopy (EDX) studies of these sheets showed that they contained Co, Zn and S. The sheets were particularly prevalent in the sulfided Co/Zn 30/70 material. Further tests were then carried out using the Co/Zn 30/70 sample in order to investigate whether these sheets were present uniformly across the absorption bed. A sample of the unsulfided absorbent was split into five 1 cm^3 beds and treated with 2% H_2S in the breakthrough apparatus until H_2S was detected from the exit of the fifth bed. The electron micrographs of beds 1, 3 and 5 are shown in Fig. 4. The micrographs of the sulfided samples clearly showed that sheet structures were most prevalent in bed 1, the top bed, less sheets were present in bed 3 and the sheets were least in evidence in bed 5, the bottom bed. The micrographs of beds 1 and 3 showed the presence of well defined semi-fused crystals surrounded by a thick sheet-like material. The micrograph of bed 5 largely resembled that of the unsulfided material but with some further loss of crystal definition. These results thus indicated that fusion of the conglomerated particles occurred on sulfiding the samples and that the crystals then became more clearly defined as the sheet-like material developed and grew.

A study of bed 3 of the sulfided Co/Zn 30/70 by electron energy loss spectroscopy (EELS) was undertaken. The results for analysis of representative samples of the particles and the sheets are presented in Fig. 5. Analysis of the particles showed that the ratio of Co/Zn was 42/58, and it remained constant on scanning across the particles. This result can be compared with atomic absorption analysis of the oxide which indicated that the Co/Zn ratio was 31/69; the sulfided particles were thus cobalt rich. EELS studies of the sheet-like material, on the other hand, showed that the Co/Zn ratio varied across the sample, but that the sheets were always zinc rich.

The FTIR spectra of the sulfided oxides were, in general, very similar to the FTIR spectra of the oxides reported previously.[15] This is not surprising, since metal–sulfur vibrations are generally of low intensity. The main bands observed for the unsulfided oxides were the OH stretch at *ca.* 3400 cm^{-1}, the OH bending mode at *ca.* 1625 cm^{-1} and a band at *ca.* 1510 cm^{-1} that could be attributed to residual carbonate. A band at 550 cm^{-1} was also observed in the zinc rich samples[15] and attributed to ZnO;[19] sharp bands observed at 588 and 575 cm^{-1} in the cobalt rich oxides were attributed

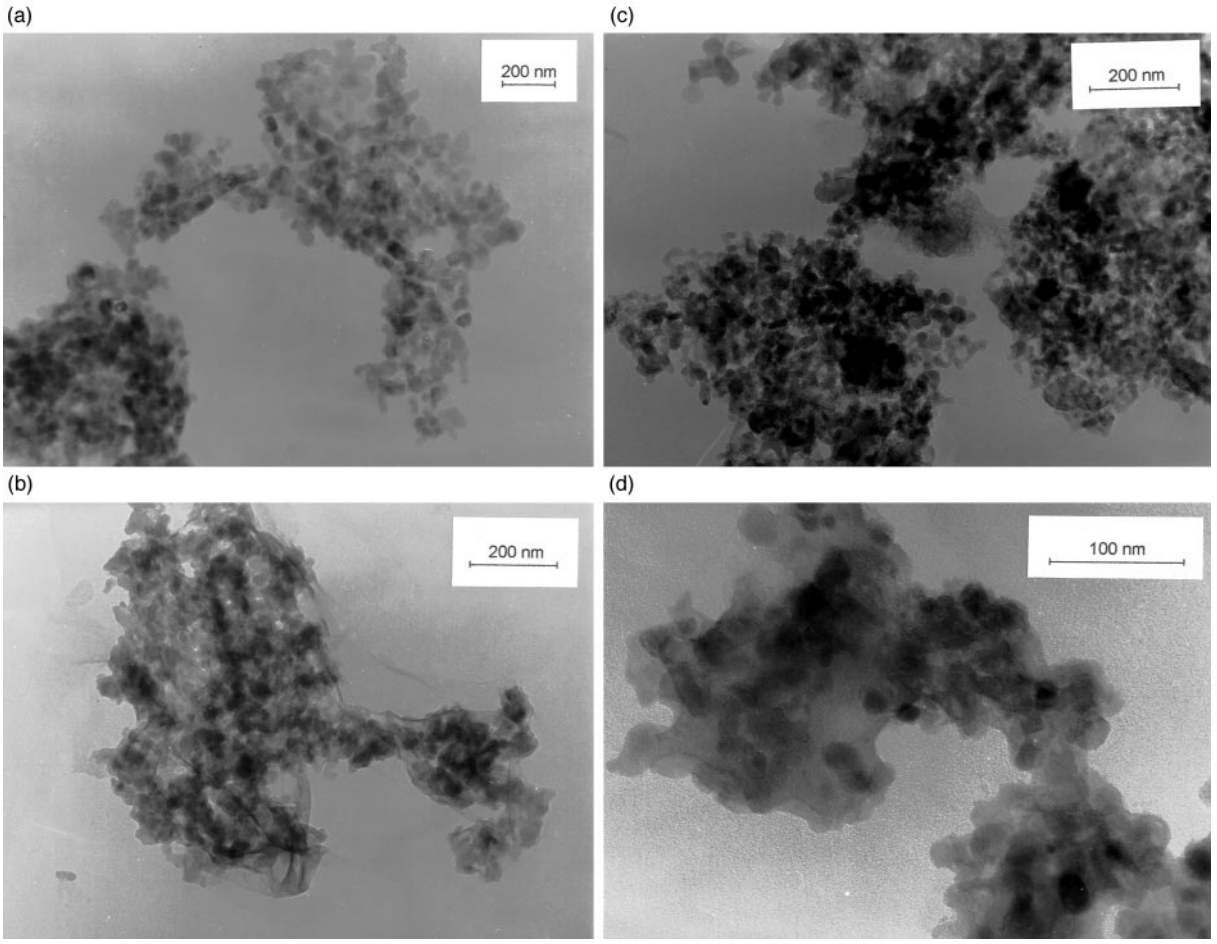

Fig. 3 Transmission electron micrographs of the sulfided oxide phases of Co/Zn: (a) 0/100, (b) 30/70, (c) 40/60, (d) 100/0.

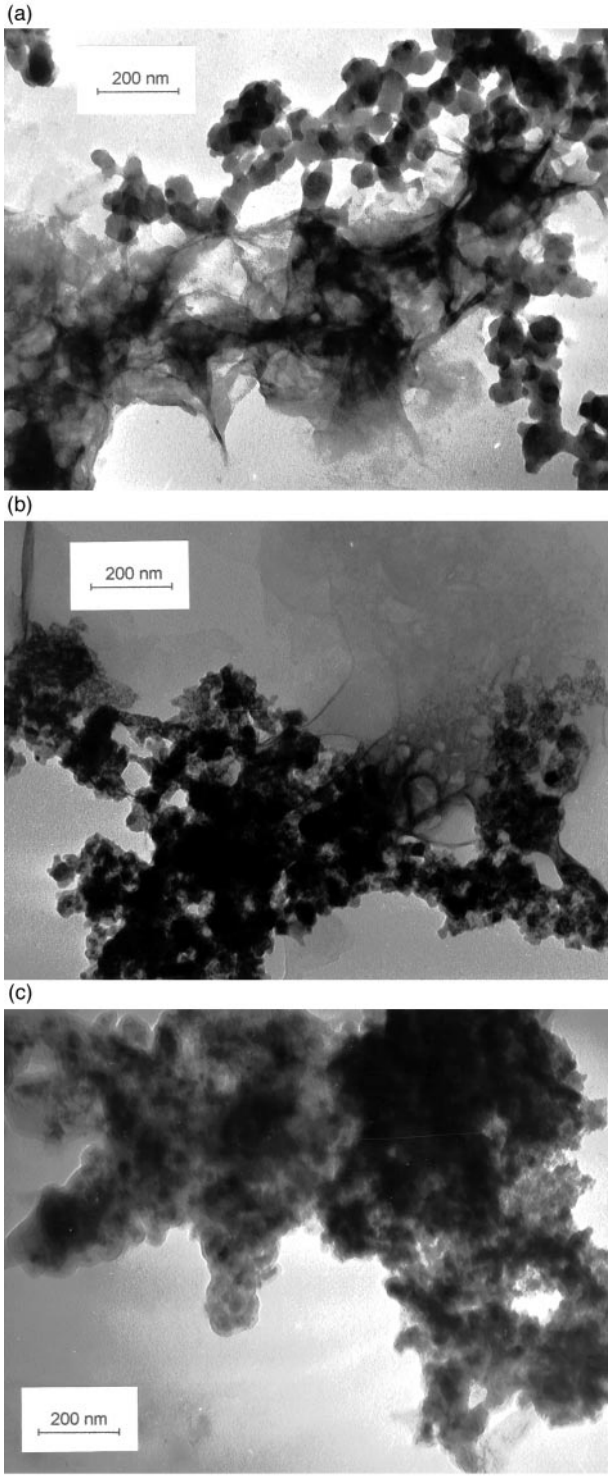

Fig. 4 Transmission electron micrographs of the split beds of the 30/70 sample after sulfidation: (a) bed 1, (b) bed 3, (c) bed 5.

to Co_3O_4.[20] No additional bands were observed in the sulfided Co/Zn 0/100 sample compared with the unsulfided oxide since the conversion to sulfide was quite low. However, the sulfided Co/Zn 10/90 sample had a low intensity peak at 1129 cm^{-1}, and a shoulder at 1180 cm^{-1}, which can be attributed to β-ZnS.[19] This was accompanied by a reduction in intensity of the two peaks characteristic of Co_3O_4. Similar results were obtained for the sulfided Co/Zn 20/80, 30/70 and 40/60 sulfided samples. The peak and shoulder attributed to ZnS was of much lower intensity for the sulfided oxides with Co/Zn ratios $\geqslant$50/50. The absence of ZnS bands from the more cobalt-rich samples could be accounted for by the formation of cobalt

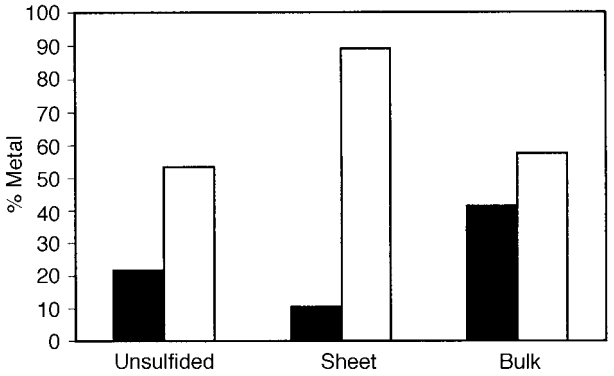

Fig. 5 Graph showing the percentage cobalt (■) and zinc (□) obtained after examination of the sheet-like material and the main body of the sulfided Co/Zn 30/70 sample by EELS. An average of four separate areas is given.

sulfides in these materials. However, it was not possible to observe cobalt sulfide in these samples, as the Co–S bands occur below the cut-off frequency of the spectrometer (400 cm^{-1}).

Surface analysis

The sulfided oxides were analysed by XPS in order to detect any changes in the surface composition of the oxides on sulfidation. The binding energies are listed in Table 2. Peak fitting using Gaussian curves gave binding energies of 1021.6 and 1019 eV. These results can be compared with those obtained for the oxides where only one peak at 1021.6 eV could be seen. This was assigned to Zn^{2+} ions in an oxide environment.[15] The lower binding energy component was thought to be due to Zn^{2+} ions bonded to sulfide.[21,22] The results listed in Table 2 show that the percentage contribution of this 'zinc sulfide' peak decreased as the Co/Zn ratio increased.

The Co $2p_{3/2}$ XP spectrum for the Co/Zn 30/70 sulfided oxide is shown in Fig. 6, and binding energies for Gaussian fitted peaks for each of the sulfided oxide samples are listed in Table 2. Assignment of the observed Co $2p_{3/2}$ spectra to cobalt oxidation states and ligand environment proved difficult, especially in the case of the Co/Zn 10/90 sample, and this was attributed to differential charging effects. Curve fitting of the Co $2p_{3/2}$ spectra for the sulfided Co/Zn 20/80, 30/70 and 40/60 samples showed that the Co $2p_{3/2}$ transition consisted of a main component with a binding energy of *ca.* 779 eV and a second component with a binding energy of *ca.* 782 eV. The low binding energy component at *ca.* 779 eV can be assigned either to Co^{3+} in an oxide environment,[23] or to

Table 2 Binding energies for the sulfided oxides. Charging effects have been referenced to the O 1s peak at E_B=530.0 eV (FWHM in parentheses)

Zn $2p_{3/2}$			Co $2p_{3/2}$		S 2p	
Co/Zn	E_B/eV	%	E_B/eV	%	E_B/eV	%
0/100	1021.6 (2.6)	72.5			161.0	3.0
	1019.6 (2.9)	27.5				
10/90	1021.4 (3.5)	78.0	780.0 (5.0)	71.6	161.5	4.6
	1024.8 (3.0)	22.0	785.1 (5.5)	28.4		
20/80	1021.6 (2.9)	86.3	779.0 (3.1)	93.4	162.5	3.1
	1019.2 (2.2)	13.7	781.6 (2.2)	6.6	168.7	4.1
30/70	1020.9 (2.7)	94.6	779.2 (3.0)	91.9	162.0	3.7
	1018.8 (1.9)	5.5	781.9 (2.2)	8.1	167.8	3.7
40/60	1021.9 (2.4)	94.0	779.3 (2.3)	69.3	162.4	2.9
	1019.8 (1.4)	6.0	781.2 (2.6)	30.7	168.7	4.7
100/0			777.8 (2.1)	74.2	161.9	2.5
			780.3 (2.8)	25.9		

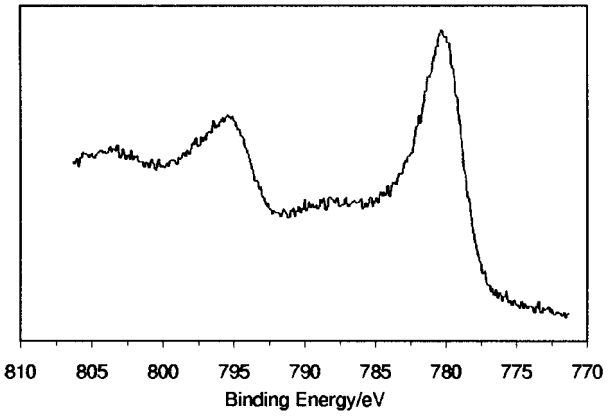

Fig. 6 The Co $2p_{3/2}$ transition for the sulfided Co/Zn 30/70 oxide.

Co^{2+} attached to a sulfide ligand.[24] The higher binding energy component at *ca.* 782 eV can be assigned to cobalt present as Co^{2+} in an oxide environment.[23] A satellite peak at *ca.* 785 eV was also observed in the sulfided Co/Zn 20/80 and 30/70 samples; this is indicative of cobalt present in the 2+ oxidation state.[15,25] These results can be contrasted with the XP spectra observed in the unsulfided material where the Co $2p_{3/2}$ was found exclusively as Co^{3+} at Co/Zn ratios $\leqslant$30/70 and this was attributed to the formation of a 'surface spinel' $ZnCo_2O_4$.[15] This implies that surface reconstruction of the oxide has occurred on sulfiding. On increasing the Co/Zn ratio from 20/80 to 30/70 and 40/60 the FWHM of the Co $2p_{3/2}$ peak with a binding energy of *ca.* 779 eV decreased from 3.1 to 3.0 and 2.3 respectively. At the same time, there was a marked increase in the sulfur uptake of these samples with increase in cobalt concentration (Table 1). This indicates that at low cobalt loadings the low binding energy feature is due to a mixture of cobalt(II) sulfide and cobalt(III) oxide, but the proportion of sulfide to oxide increases with increasing cobalt concentration. Indeed, this is borne out by an analysis of the sulfided Co/Zn 100/0 Co $2p_{3/2}$ spectrum where curve fitting showed that the Co $2p_{3/2}$ transition consisted of a main component with a binding energy of 777.8 eV and a second component at *ca.* 780.3 eV. The low binding energy component of this spectrum had a FWHM of 2.1 and the binding energy is typical of that expected for Co^{2+} ions in a sulfide environment.[24] This is in accordance with the fact that this sample had reacted almost stoichiometrically with H_2S. The higher binding energy feature is typical of Co^{3+} in an oxide environment.[23]

The S $2p_{3/2}$ XP spectra for all the sulfided oxides were studied and are shown in Fig. 7. The S $2p_{3/2}$ transition for all the samples gave a peak with a binding energy of *ca.* 161.0 eV which could be assigned to S^{2-}.[21,24] The sulfided oxides with Co/Zn ratios of 20/80, 30/70 and 40/60 also had an additional minor peak in their S $2p_{3/2}$ spectra at *ca.* 167 eV. The intensity of this minor peak increased with increase in cobalt concentration (Table 2), and it was attributed to sulfur present as sulfate.[26] Curve fitting also indicated the presence of a small higher binding energy feature in the sulfided Co/Zn 100/0 sample which was also likely to be due to sulfate formation. However, it was difficult to assign this unambiguously due to differential charging.

Quantitative analyses of the S $2p_{tot}$/Zn $2p_{3/2}$ and S $2p_{tot}$/Co $2p_{3/2}$ ratios for each of the sulfided oxides were determined as outlined in the experimental section and are presented in Table 3. The sulfur data were analysed as S $2p_{tot}$ as it was not possible to separate the S $2p_{1/2}$ and S $2p_{3/2}$ peaks. The quantitative data for sulfur will thus be overestimated. As mentioned previously, the data will thus be used only to indicate trends in the sulfur/metal ratios in the series of sulfided oxides. The H_2S breakthrough tests had shown that the sulfur

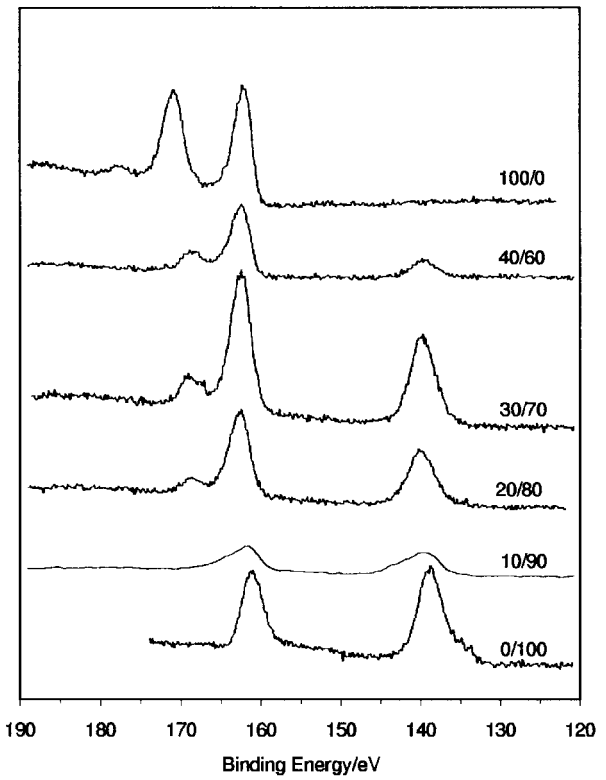

Fig. 7 The S 2p transitions at *ca.* 167 eV for the sulfided oxides. The peak at 139 eV is due to Zn 3s.

Table 3 Quantitative analyses for the sulfided oxides

Co/Zn	S $2p_{Tot}$/Zn $2p_{3/2}$	S $2p_{Tot}$/Co $2p_{3/2}$
0/100	0.499	
10/90	0.946	6.467
20/80	0.822	2.638
30/70	1.136	3.447
40/60	2.400	2.281
100/0		2.107

absorption capacity calculated as the % reaction for each absorbent increased with increase in cobalt loading. The XPS studies showed that the S $2p_{tot}$/Zn $2p_{3/2}$ ratio, with the exception of the sulfided Co/Zn 10/90 sample, also increased with increase in sulfur uptake. However, the S $2p_{tot}$/Co $2p_{3/2}$ ratio reached a maximum at a Co/Zn ratio of 30/70 and declined at higher cobalt loadings. This indicated that most of the sulfur was associated either with the zinc component or a Co/Zn solid solution in the sulfided mixed oxides. The decrease in the low binding energy feature of zinc with increase in sulfur content which was accompanied by a narrowing of the Co $2p_{3/2}$ peak width with increasing cobalt loading indicated that the sulfur was associated with the mixed phase rather than a zinc phase alone. The decline in the S $2p_{tot}$/Co $2p_{3/2}$ ratio at cobalt concentrations above Co/Zn 30/70 can be attributed to surface reconstruction. A slight anomaly to these trends was observed in the case of the sulfided Co/Zn 10/90 sample in that the S $2p_{tot}$/Zn $2p_{3/2}$ and S $2p_{tot}$/Co $2p_{3/2}$ ratios were high compared with those observed for the sulfided Co/Zn 0/100 and 20/80 samples. This indicated that the sulfur is concentrated on the surface of the Co/Zn 10/90 sample. The S $2p_{tot}$/Co $2p_{3/2}$ ratio for the sulfided Co/Zn 100/0 sample was 2:1, indicating that there was a small excess of sulfur at the surface.

Discussion

The main aim of our work has been to synthesise high surface area absorbents for the efficient removal of H_2S at low temperatures. In these 'breakthrough' tests it is the initial rather than the equilibrium rate of absorption that is measured. H_2S is known to be dissociated into H^+ and HS^- on a zinc oxide surface.[27] The subsequent reaction is then controlled by either pore or lattice diffusion. In the pore diffusion limitation, the rate of reaction will be controlled by the rate of diffusion of HS^- in the pores to fresh oxide. It will thus be controlled by both the initial pore size and pore accessibility as the reaction proceeds, *i.e.* the absence of blockages during sulfide formation in the pores. In lattice diffusion, HS^- reacts with oxide at the surface and the sulfided surface is then replenished by migration of fresh oxide to the sulfided surface. The rate of reaction is thus controlled by the diffusion of HS^- into the oxide lattice and migration of oxide and water to the surface. An inert sulfide shell is formed which reduces the rate of diffusion of fresh absorbent such that 'breakthrough' occurs when the rate of replenishment of the surface is less than the rate of reaction.[28,29] It is likely that lattice diffusion controlled the rate of sulfidation of the samples with Co/Zn ratios $\leqslant$40/60, since the % reaction increased linearly with increase in surface area (Fig. 1). These oxides had a predominantly ZnO structure for the bulk with increasing quantities of the spinel $ZnCo_2O_4$ present at the surface.[15] Furthermore, the % reaction was found to increase with increase in % cobalt in the absorbents (Fig. 2), indicating that at Co/Zn ratios $\leqslant$40/60 the main function of the cobalt was to increase the available area for reaction with H_2S. The depth of reaction was calculated for each absorbent, assuming a concentration of 1×10^{19} ZnO ion pairs m^{-2} and 1.51×10^{19} cobalt ions m^{-2},[11,30] and the results are presented in Table 1. These calculations showed that the depth of reaction amounted to *ca.* 3 monolayers, and this again is an indication that lattice diffusion is the rate limiting factor. A similar mechanism has also been found to operate in measurements of the initial rates of sulfidation of zinc oxide at low temperatures.[27]

The data in Fig. 1 and 2 for the sulfidation of the Co/Zn 50/50 sample showed that the surface area and % reaction were lower than would be expected for its composition. Differential thermal analysis (DTA) indicated that a large exothermic transition occurred on decomposition of the precursor to the oxide.[15] This may have induced some localised particle sintering resulting in a lowering of the surface area, and consequently the % reaction would also be lower.

The best absorbents for H_2S were the oxides with Co/Zn ratios of 70/30, 90/10 and 100/0. They adopted either a single phase zincian Co_3O_4 (Co/Zn 70/30 and 90/10) or a pure Co_3O_4 (Co/Zn 100/0) spinel structure. The % reaction increased markedly with surface area and % cobalt concentration (Fig. 1 and 2). The oxide with the Co/Zn 100/0 ratio was the best absorbent, reacting almost stoichiometrically with H_2S at 30 °C. Since the reaction depth was only 3.7 monolayers, this absorbent was quite porous and one quarter of all the available reaction sites were on the surface. The greater sulfur uptake by absorbents with the Co_3O_4 structure can be understood on both thermodynamic and structural terms. Thermodynamically, Co_3O_4 has a lower free energy for sulfidation than ZnO,[11] and sulfiding the cubic Co_3O_4 normal spinel to its sulfided equivalent, the spinel Co_3S_4, or Co_8S_9 which has a defective rock salt structure, will require less rearrangement of the lattice than the conversion of hexagonal ZnO to the cubic ZnS.

XPS analysis of the mixed oxides had shown that all the surface cobalt was present as $ZnCo_2O_4$ at Co/Zn ratios of $\leq$30/70. Analysis of the unsulfided oxides had also shown that there was an increase in the ionic charge of the Co^{3+} ions with increase in cobalt loading up to a Co/Zn ratio of 40/60. This was the point at which Co^{2+} was first detected at the surface of the oxides.[15] This high ionic charge was retained as the cobalt loading was increased further. The ionic charge of Zn^{2+} decreased with increase in cobalt loading. There was thus an increased electrostatic gradient at the surface with increase in cobalt loading. TEM (Fig. 3 and 4) and EELS studies (Fig. 5) had indicated that zinc-rich sheet like material was formed after sulfiding the mixed oxides, and XPS studies had shown that both Co^{2+} and Co^{3+} ions were present at the surface after sulfidation in oxides where only the spinel $ZnCo_2O_4$ had previously been found at the surface. These results indicate that surface reconstruction occurred on sulfiding the mixed oxides. The driving force for surface reconstruction would be the high electrostatic gradient and the stability attained by the replacement of weak substrate bonds by strong adsorbate–substrate bonds.[31] Surface segregation of the oxide phases would then occur, and thin sheet-like material would grow at the surface of the absorbent. It is interesting to observe that the sheets formed on the reconstructed surfaces were zinc rich, yet thermodynamically the free energy of formation of ZnS from ZnO is less favourable than that of the cobalt sulfide from Co_3O_4. It should be noted however that some cobalt was required for this process to occur since no sheet-like structures were observed on sulfiding the Co/Zn 0/100 material. H_2S absorption may take place on the mixed oxides, but preferential sulfiding of the zinc oxide may occur since the bulk thermodynamic properties are not necessarily reflected in the behaviour of the surface sulfides. Indeed, the free energies of formation of surface sulfides have been reported to be *ca.* 50 kJ mol^{-1} metal more favourable than their bulk sulfides.[1] No sheet-like material was observed in the sulfided oxide with the composition Co/Zn 100/0, implying that surface reconstruction only occurs in the mixed oxides.

XPS studies of the sulfided oxides also observed that a S 2p peak specific to SO_4^{2-} was present in those oxides with Co/Zn ratios $>$10/90 which had a 'surface spinel' $ZnCo_2O_4$ or zincian Co_3O_4 present prior to sulfiding. Previous studies have shown that when a mixed oxide system is sulfided, separation of the two oxide components into two distinct phases can occur.[32] It is likely therefore that cobalt(II) and cobalt(III) oxides and ZnO would be segregated from $ZnCo_2O_4$ or zincian Co_3O_4 on sulfiding, and that H_2S would act as a reducing agent forming sulfur which would be oxidised to sulfate on exposure to air.

$$3ZnCo_2O_4 + H_2S \rightarrow 3ZnO + 2Co_3O_4 + H_2O + S$$

$$Co_3O_4 + H_2S \rightarrow 3CoO + H_2O + S$$

$$CoO + H_2S \rightarrow CoS + H_2O$$

$$ZnO + H_2S \rightarrow ZnS + H_2O$$

The efficiency of the reconstruction in replenishing the surface may also have contributed to the improved sulfur uptake of the cobalt-rich absorbents. The sulfided Co/Zn 100/0 material was the best absorbent since the transport of adsorbed HS^- into the bulk of the solid was more efficient than in the sulfided zinc-containing oxides and the reaction between H_2S and Co_3O_4 is both thermodynamically favoured over that between H_2S and ZnO and requires less structural rearrangement on sulfiding the oxide.

Acknowledgements

We are grateful to the EPSRC and ICI Katalco for supporting this work.

References

1 C. H. Bartholomew, P. K. Agrawal and J. R. Katzer, *Adv. Catal.*, 1982, **31**, 135.
2 P. O'Neill, *Environmental Chemistry*, Chapman and Hall, London, 2nd edn., 1993.

3 P. J. H. Carnell and P. E. Starkey, *Chem. Eng.*, 1984, **408**, 30.
4 P. R. Westmoreland and D. P. Harrison, *Environ. Sci. Technol.*, 1976, **10**, 659.
5 P. R. Westmoreland, J. B. Gibson and D. P. Harrison, *Environ. Sci. Technol.*, 1977, **11**, 488.
6 J. M. Cognion, *Chim. Ind. Gen. Chim.*, 1972, **105**, 757.
7 G. U. Hopton and R. H. Griffith, *Gas J.*, 1946, **247**, 4311.
8 J. E. Garside and R. F. Phillips, *A Textbook of Pure and Applied Chemistry*, ed. S. C. Laws, Pitman and Sons, London, 1962, p. 590.
9 K. Eddington and P. Carnell, *Oil Gas J.*, 1991, **89**, 69.
10 G. W. Spicer and C. Woodward, *Oil Gas J.*, 1991, **89**, 76.
11 T. Baird, P. J. Denny, R. W. Hoyle, F. McMonagle, D. Stirling and J. Tweedy, *J. Chem. Soc.*, *Faraday Trans.*, 1992, **88**, 3375.
12 T. Baird, K. C. Campbell, P. J. Holliman, R. W. Hoyle, D. Stirling and B. P. Williams, *J. Chem. Soc.*, *Faraday Trans.*, 1996, **92**, 445.
13 T. Baird, K. C. Campbell, P. J. Holliman, R. W. Hoyle, D. Stirling and B. P. Williams, in *Recent advances in oilfield chemistry*, ed. P. H. Ogden, RSC Publication, Cambridge, UK, 1994, pp. 234–250.
14 T. Baird, K. C. Campbell, P. J. Holliman, R. W. Hoyle, D. Stirling and B. P. Williams, *J. Chem. Soc.*, *Faraday Trans.*, 1995, **91**, 3219.
15 T. Baird, K. C. Campbell, P. J. Holliman, R. W. Hoyle, D. Stirling, B. P. Williams and M. Morris, *J. Mater. Chem*., 1997, **7**, 319.
16 J. H. Schofield, *J. Electron Spectrosc. Relat. Phenom.*, 1976, **8**, 129.
17 D. Briggs and M. P. Seah, *Practical Surface Analysis by Auger and XPS*, Wiley, Chichester, 1985.
18 N. G. Farr and H. J. Griess, *J. Electron Spectrosc. Relat. Phenom.*, 1989, **49**, 293.
19 J. Ferraro, *Low Frequency Vibrations of Inorganic and Coordination Compounds*, Plenum Press, New York, 1971.
20 J. A. Gadsden, *Infrared Spectra of Minerals and Related Inorganic Compounds*, Butterworths, London, 1975.
21 G. Deroubaix and P. Marcus, *Surf. Interface Anal.*, 1992, **18**, 39.
22 S. W. Gaarenstroom and N. Winograd, *J. Chem. Phys.*, 1977, **67**, 3500.
23 J. J. Chuang, C. R. Brundle and D. W. Rice, *Surf. Sci.*, 1976, **59**, 413.
24 I. Alstrup, I. Chorkendorff, R. Candia, B. S. Clausen and H. Topsoe, *J. Catal.*, 1982, **77**, 397.
25 R. B. Moyes and M. W. Roberts, *J. Catal.*, 1977, **49**, 216.
26 C. D. Wagner, in *Handbook of X-Ray and Ultraviolet Photoelectron Spectroscopy*, ed. D. Briggs, Heyden, London, 1978.
27 C. H. Lawrie, PhD Thesis, Edinburgh, 1991.
28 P. J. H. Carnell and P. J. Denny, *AICHE Ammonia Safety Symp.*, 1984, 99.
29 Yu. V. Furmer, V. S. Beskov, O. I. Brui, V. V. Yudina and M. L. Danstig, *Sov. Chem. Ind.*, 1982, **14**, 1499.
30 J. R.Anderson and K. C. Pratt, *Introduction to Characterisation and Testing of Catalysts*, Academic Press, London, 1985.
31 G. A. Somorjai, *Introduction to Surface Chemistry and Catalysis*, Wiley-Interscience, New York, 1994.
32 R. V. Siriwardane and J. A. Poston, *Appl. Surf. Sci.*, 1990, **45**, 841.

Paper 8/06909C